Available online at www.sciencedirect.com
SCIENCE DIRECT®
ELSEVIER
International Journal of Solids and Structures 43 (2006) 2744–2760
INTERNATIONAL JOURNAL OF SOLIDS and STRUCTURES
www.elsevier.com/locate/ijsolstr

Scaling impacted structures when the prototype and the model are made of different materials

Marcílio Alves *, Roberto Eiki Oshiro

Group of Solid Mechanics and Structural Impact, Department of Mechatronics and Mechanical Systems Engineering, University of São Paulo, São Paulo 05508-900, Brazil

Received 26 January 2005; received in revised form 2 March 2005
Available online 13 April 2005

Abstract

By properly applying scaling laws, it is possible to infer the behaviour of a structure from the response of a similar model whose dimensions are scaled by a factor β. In some cases, however, e.g. in the case of strain rate sensitive structures under severe dynamic loads, these laws become distorted, severely limiting this approach. In this article, a methodology for the correction of this distortion is explored for the case when the structure and the model are made of different materials. It is shown that the behaviour of a structure, say, made of mild steel, can be forecast from the response of a model, say, made of aluminium. The technique here detailed is shown to be valid for simple structures subject to axial and transverse impact loads.

Keywords: Scaling; Structural impact; Different materials

1. Introduction

Scaling models for structural analysis has been less used nowadays due to the extensive availability of sophisticated finite element programmes. These computer programmes can perform complex structural analysis with a high accuracy provided material behaviour, boundary and initial conditions as well as geometry are known.

Nevertheless, there are many instances where experimental validation of a structure, performance is necessary. As an example, extensive bird impact tests against an aircraft fuselage needs to be performed in order to commission the structure. Tests in such large structures can be quite complex and expensive

* Corresponding author. Tel.: +55 11 3091 5757; fax: +55 11 3091 5461.
E-mail address: maralves@usp.br (M. Alves).

0020-7683/$ - see front matter
doi:10.1016/j.ijsolstr.2005.03.003

and to avoid them one can test a model identical to the actual structure except for its dimensions, which are scaled by a single factor, β. It is said in this case that the model and the structure (or prototype) are geometrically scaled.

Of course, if the prototype response is to be inferred from the model behaviour, the loads applied to the latter should also be scaled. To this end, there is a systematic way to find out how the measured variables and applied loads in a model can be correlated with the ones in the prototype.

To fix ideas, consider an elastic wave travelling on a prototype and on a model. If they are made from the same material, the wave speed, c, will be the same in both structures such that the time, T, for the wave to propagate a distance L in the prototype is

$$T = \frac{L}{c}. \tag{1}$$

In the model, scaled by

$$\beta = \frac{l}{L}, \tag{2}$$

the time, t, for the wave to propagate a distance l is given by

$$t = \frac{l}{c} = \frac{\beta L}{c}, \tag{3}$$

such that

$$t = \beta T. \tag{4}$$

Using a similar reasoning for other variables, one can obtain Table 1, which lists how a variable in the model can be related to its correspondent in the prototype. Observe from this table that the strain rate in a model is $1/\beta$ times larger than the strain rate in a prototype, whereas the stresses are the same.

In order to exemplify that the scaling laws are valid for complex loading cases, consider a tube axially impacted by a dropping mass. This problem was modelled by the authors using the finite element method as implemented in the software ABAQUS. The tube is clamped on its base and has a diameter of 20 mm, wall thickness of 1 mm and height of 300 mm. The material is elastic, perfectly plastic with an elastic modulus of 210 GPa, Poisson ratio of 0.33, mass density of 7800 kg/m^3 and flow stress of 235 MPa. These material characterisitcs represent a mild steel but it is remarked that strain rate effects were not taken into account in the simulation at this stage. An energy of 2 kJ was applied to the tube by means of a mass of $G = 4.44$ kg hitting it at a speed of $V_0 = 20$ m/s. Gravity effects were not considered.

Fig. 1(a) shows the shell final configuration, i.e. after all the mass kinetic energy was dissipated.

Table 1
Relationships between the model and the prototype for some variables

Variable	Scaling
Length (L)	β
Mass (G)	β^3
Stress (σ)	1
Time (t)	β
Velocity (V)	1
Displacement (δ)	β
Strain (ε)	1
Acceleration (A)	$1/\beta$
Strain rate ($\dot{\varepsilon}$)	$1/\beta$

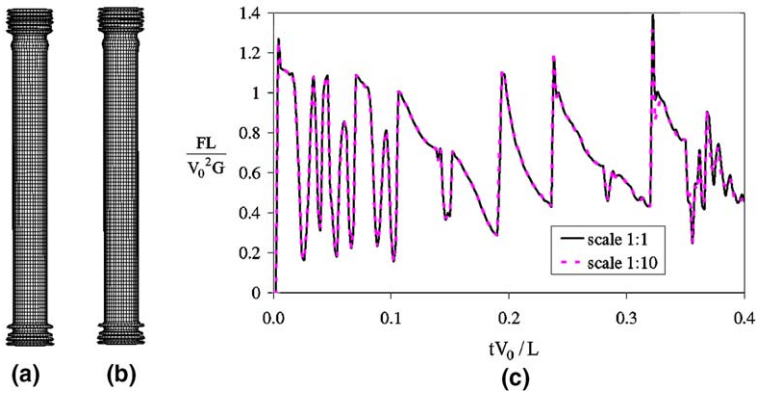

Fig. 1. Final configuration and load profile of a tube under axial impact: (a) prototype, (b) model 10 times smaller but enlarged 10 times for better visualisation, (c) dimensionless load times displacement for the model and the prototype.

Another tube scaled by a factor $\beta = 1/10$ was also simulated, and from Table 1, it can be seen that the impact velocity should be the same but the impact mass should be $\beta^3 G = 0.00444$ kg such that the input energy is now 2 J. By so proceeding, one obtains the deformed tube in Fig. 1(b), which has been enlarged $1/\beta = 10$ times in order to be visible.

It is evident that the original tube and its reduced model are exactly the same, which is further corroborated by the dimensionless load–time behaviour in Fig. 1(c), where the variables were scaled as noted. The reason for this similar behaviour is that all the variables involved in the phenomenon obey the scaling laws and so the behaviour of the prototype can be inferred from the model response.

However, this is not always the case when some other peculiarities of the impact phenomenon are taken into account. For instance, it is well known that when strain rate effects influence the material behaviour and, hence, the structure response, the model and the prototype will generally not scale.

To better examine this point, consider the constitutive relation which predicts how the static flow stress in the prototype, σ_{s_p}, is increased by the strain rate, $\dot{\varepsilon}_p$

$$\sigma_{d_p} = \sigma_{s_p}\left[1 + \left(\frac{\dot{\varepsilon}_p}{D}\right)^{1/q}\right], \tag{5}$$

where D and q are material constants and the subscripts d, s and p stand for dynamic, static and prototype (Alves, 2000).

Observe from Table 1 that the strain rate in the model, m, is

$$\dot{\varepsilon}_m = \dot{\varepsilon}_p/\beta, \tag{6}$$

such that the model to prototype stress ratio gives

$$\frac{\sigma_{d_m}}{\sigma_{d_p}} = \frac{\left\{1 + \left(\frac{\dot{\varepsilon}_m}{D}\right)^{1/q}\right\}}{\left\{1 + \left(\frac{\dot{\varepsilon}_p}{D}\right)^{1/q}\right\}} = \frac{\left\{1 + \left(\frac{\dot{\varepsilon}_p}{\beta D}\right)^{1/q}\right\}}{\left\{1 + \left(\frac{\dot{\varepsilon}_p}{D}\right)^{1/q}\right\}}, \tag{7}$$

which clearly varies with the scaling factor, β, and the strain rate, for a given set of material constants, as pointed out by Oshiro and Alves (2004).

Since the dynamic stress ratio depends on the scaling factor, it violates the usual scaling laws which require the stress in a model and in a prototype to be invariant, according to Table 1. This dependence can be

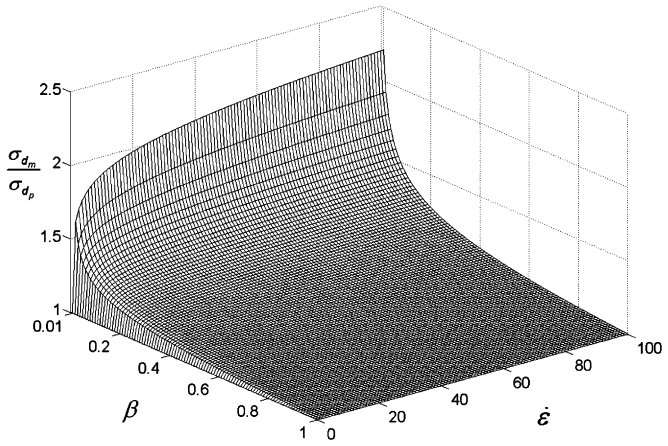

Fig. 2. Model to prototype stress ratio versus the scaling factor and strain rate for mild steel.

quite significant, as exemplified in Fig. 2, for a range of strain rates and scaling factors when adopting $D = 40/\text{s}$ and $q = 5$, which are typical values for mild steel.

To demonstrate that the strain rate affects the scaling laws, consider the same tube which was simulated before but now taking into account the influence of the strain rate on the material response when adopting $D = 40/\text{s}$ and $q = 5$. The tube is clamped at its bottom and the impact velocity and mass are 60 m/s and 1.944 kg, giving a total input energy of 3.5 kJ. Fig. 3(a) presents the final configuration of the prototype,

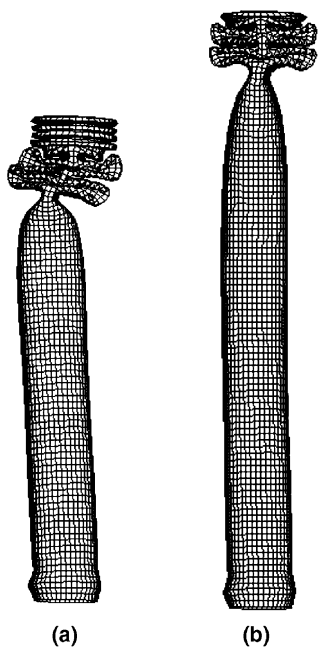

Fig. 3. Final configuration of a strain rate sensitive shell under axial impact: (a) prototype and (b) model 10 times smaller (the figure was enlarged 10 times for better visualisation).

while Fig. 3(b) shows the tube scaled by a factor $\beta = 1/10$ (the figure is again enlarged $1/\beta$ times). It is clear that the model behaves quite distinctly from the prototype and the reason is solely due to the strain rate effects.

When comparing Figs. 1 and 3, it is evident that the scaling laws fail to represent the prototype behaviour when strain rate effects are considered. Of course, the same can be said when the prototype and the model are made from different materials.

This problem of non-scalability of the stresses due to the non-linear material response to strain rates is crucial when dealing with the impact of structures in scaled models. Many authors have investigated the problem of scaling impacted structures (Baker et al., 1991; Booth et al., 1983; Wen and Jones, 1993; Nurick and Martin, 1989; Duffey et al., 1984; Jones, 1984; Jones et al., 1984) and some scaling numbers have been proposed in the literature (Johnson, 1973; Nurick and Martin, 1989; Zhao, 1998), with Li and Jones (2000) critically discussing them. Also, Hu (2000), Shi and Gao (2001) and Jacob et al. (2004) applied scaling numbers to the analysis of plates and shells.

Scaling strain rate sensitive structures have recently received attention by the authors (Oshiro and Alves, 2004; Alves and Oshiro (in press)). The authors have applied a simple dimensional analysis, as outlined in Baker et al. (1991) and Jones (1989), but using an alternative dimensionless basis to the common MLT (mass, length, time) basis. The Authors were able to suggest a methodology for correcting strain rate effects, such that a rational way was devised to change the impact or blast velocity in a way that models and prototypes follow the scaling laws. Also, Alves and Oshiro (in press), have shown a procedure to obtain the model impact mass for a strain rate sensitive structure such that the model and the prototype behave the same.

In dealing with the problem of predicting the behaviour of a real structure from the behaviour of a model, clearly, the prototype and the model should be made from the same material, but this can be quite difficult to achieve in many cases. It is likely that a prototype made of a steel plate 10 mm thick and its model, say 20 times smaller and hence made of a 0.5 mm thick steel plate, will exhibit different material properties due to the possible different manufacturing processes of the core material. Such a difference can result in a model behaving in a way that it makes it quite difficult to infer from it the desired prototype response.

In considering the above issues, this article further expands the methodology in Oshiro and Alves (2004) and Alves and Oshiro (in press) to the case where the model is made of a different material from that of the prototype. By so proceeding, it is possible to predict, in an extreme case, the strain rate sensitive prototype behaviour from a non-strain rate sensitive model response. Likewise, within certain limitations to be discussed later, it is possible to infer the behaviour of a prototype made from metal by analysing the response of a plastic model.

The correction procedure is outlined in the next section, starting with strain rate sensitive structures, as described in detail by Oshiro and Alves (2004) and Alves and Oshiro (in press), and expanding it to the case of dissimilar materials. Section 3 applies the correction procedure to the problem of the impact of a mass on a clamped beam, followed by the problem of a beam under a blast load. In Section 5, the axial impact of a double plate structure is analysed. The subsequent section discusses the results, all showing that it is indeed possible to correct the distortion of the scaling laws. The major conclusions in Section 7 closes the article.

2. Correcting scaling laws when the model and the prototype are made from different materials

The methodology devised by the authors for correcting the distortion of scaling laws is based on the use of a dimensionless basis formed not by mass, time and length, as have always been used in structural impact mechanics, but by the impact mass, G, the initial impact velocity, V_0, and the dynamic flow stress, σ_d. From this basis, one can express all the relevant variables of an impact phenomenon, such that, for instance, time becomes

$$T = \frac{G^{1/3}}{V_0^{1/3}\sigma_{\mathrm{d}}^{1/3}}. \tag{8}$$

Other variables, such as acceleration, A, displacement, δ, strain rate, $\dot{\varepsilon}$, and stress, σ, can be obtained as shown in Table 2, which allows us to generate the following dimensionless Π terms:

$$\underbrace{\left[\frac{A^3 G}{V_0^4 \sigma_{\mathrm{d}}}\right]}_{\Pi_1}, \underbrace{\left[\frac{T^3 \sigma_{\mathrm{d}} V_0}{G}\right]}_{\Pi_2}, \underbrace{\left[\frac{\delta^3 \sigma_{\mathrm{d}}}{G V_0^2}\right]}_{\Pi_3}, \underbrace{\left[\dot{\varepsilon}\left(\frac{G}{\sigma_{\mathrm{d}} V_0}\right)^{1/3}\right]}_{\Pi_4}, \underbrace{\left[\frac{\sigma}{\sigma_{\mathrm{d}}}\right]}_{\Pi_5}. \tag{9}$$

Accordingly, the behaviour of a prototype can be inferred from these dimensionless numbers and from the scaled model response if there were no distortion. As already pointed out, one source of distortion is the material strain rate sensitivity and a way to correct it is as follows:

Define a scaling factor for the dynamic stress as

$$\beta_{\sigma_{\mathrm{d}}} = \frac{\sigma_{\mathrm{d_m}}}{\sigma_{\mathrm{d_p}}} = \frac{f(\dot{\varepsilon}_{\mathrm{m}})}{f(\dot{\varepsilon}_{\mathrm{p}})}, \tag{10}$$

where f is a generic function given by the material constitutive law. Now, the impact velocity would be the same in both the model and the prototype, according to Table 1, if it were not for the material strain rate sensitivity. To avoid the alluded distortion one writes

$$\beta_{V_0} = \frac{V_{0_{\mathrm{m}}}}{V_{0_{\mathrm{p}}}}. \tag{11}$$

The dimensionless number Π_3 from Eq. (9) leads to

$$\frac{\Pi_{3_{\mathrm{m}}}}{\Pi_{3_{\mathrm{p}}}} = \frac{\beta_\delta^3 \beta_{\sigma_{\mathrm{d}}}}{\beta_G \beta_{V_0}^2} = \frac{\beta^3 \beta_{\sigma_{\mathrm{d}}}}{\beta^3 \beta_{V_0}^2} = 1 \tag{12}$$

and so

$$\beta_{\sigma_{\mathrm{d}}} = \beta_{V_0}^2. \tag{13}$$

Also,

$$\beta_{\dot{\varepsilon}} = \frac{\dot{\varepsilon}_{\mathrm{m}}}{\dot{\varepsilon}_{\mathrm{p}}}, \tag{14}$$

but it is rewritten as

$$\beta_{\dot{\varepsilon}} = \frac{\dot{\varepsilon}_{\mathrm{m}}^{\mathrm{c}}}{\dot{\varepsilon}_{\mathrm{p}}}, \tag{15}$$

since one seeks the correct (superscript c) strain rate. Furthermore,

Table 2
A new dimensional matrix

Basis	Variables				
	A	T	δ	$\dot{\varepsilon}$	σ
V_0	4/3	−1/3	2/3	1/3	0
σ_{d}	1/3	−1/3	−1/3	1/3	1
G	−1/3	1/3	1/3	−1/3	0

$$\beta_{\dot{\varepsilon}} = \frac{\beta_{V_0}}{\beta} \tag{16}$$

can be obtained from $\Pi_{4_m}/\Pi_{4_p} = 1$, yielding

$$\beta_{\dot{\varepsilon}} = \frac{\beta_{V_0}\dot{\varepsilon}_m^{nc}}{\dot{\varepsilon}_p}, \tag{17}$$

where superscript nc stands for non-correct.

Finally, using Eq. (16), it can be shown that

$$\dot{\varepsilon}_p = \beta\dot{\varepsilon}_m^{nc}, \tag{18}$$

which allows for the calculation of the new (corrected) β_{V_0}

$$\beta_{V_0} = \sqrt{\beta_{\sigma_d}} = \sqrt{\frac{\sigma_{d_m}}{\sigma_{d_p}}} = \sqrt{\frac{f(\dot{\varepsilon}_m^c)}{f(\dot{\varepsilon}_p)}} = \sqrt{\frac{f(\beta_{V_0}\dot{\varepsilon}_m^{nc})}{f(\beta\dot{\varepsilon}_m^{nc})}}. \tag{19}$$

Observe that the approach here sets a way to correct the initial impact velocity so that the strain rate and the dynamic flow stress are properly altered. The particular form of the constitutive model, as described by the function f, is not relevant in the methodology developed here.

The correction procedure implies that the model, scaled by β, needs to be simulated so that the strain rate in its various parts can be used to obtain the stress levels and β_{σ_d}. Eq. (19) is then applied so β_{V_0} and hence the new velocity is determined. With this new velocity, the model is once more analysed and its response will now be properly scaled so that, for instance, the prototype acceleration will be $1/\beta$ the one in the corrected model, as is desired. Note that the procedure described above does not rely on any data from the prototype; the results of the full scaled structure are forecasted solely from the model response.

The methodology described above for correcting the distortion in the scaling laws due to strain rate effects can readily be expanded to the case where the model and the prototype are made from different non-strain rate sensitive materials.

Considering Eq. (19), it can be rewritten using Eq. (5) as

$$\beta_{V_0} = \sqrt{\beta_{\sigma_d}} = \sqrt{\frac{\sigma_{s_m}\left[1 + \left(\frac{\dot{\varepsilon}_m}{D}\right)^{1/q}\right]}{\sigma_{s_p}\left[1 + \left(\frac{\dot{\varepsilon}_p}{D}\right)^{1/q}\right]}}. \tag{20}$$

For materials which exhibit a low strain rate sensitivity, D is very large, which renders Eq. (20) as

$$\beta_{V_0} = \sqrt{\frac{\sigma_{s_m}}{\sigma_{s_p}}}. \tag{21}$$

Hence, Eq. (21) is to be used for non-strain rate sensitive structural problems but when the prototype and the model are made of different materials.

Eq. (20) can also be reduced to

$$\beta_{V_0} = \sqrt{\frac{\sigma_{s_m}}{\sigma_{s_p}\left[1 + \left(\frac{\dot{\varepsilon}_p}{D}\right)^{1/q}\right]}}, \tag{22}$$

for the case when the prototype material is strain rate sensitive and the model is not.

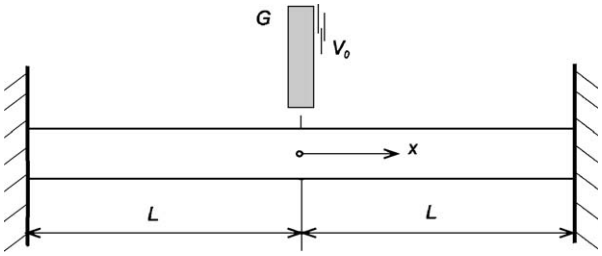

Fig. 4. Clamped beam struck by a mass, G, travelling with a velocity V_0.

In this article, one seeks to show that the response of a strain rate sensitive prototype can be obtained by examining the response of a non-strain rate sensitive model. Accordingly, Eqs. (20)–(22) will be used throughout this article to explore the validity of the methodology advocated here, applied to three different structural problems, as follows:

3. Clamped beam struck by a mass at mid-span

In order to apply the methodology described above, a clamped beam hit by a mass is considered. The beam has a rectangular cross-section of dimensions B and H, length $2L$, struck at its mid-span by a mass, G, travelling with a velocity V_0, Fig. 4. The response of this class of beams has been studied by many authors (Alves and Jones, 2002a,b; Jones, 1989) and it is relevant in terms of engineering application.

It is sought to obtain the response of a full scale strain rate sensitive mild steel beam, represented by its mid-displacement, from the results of small scale aluminium beams, with the material properties given in Table 3.

A theoretical solution for this problem was developed by Liu and Jones (1988), who obtained a final beam mid-span displacement, W_f, according to

$$w_f = \frac{W_f}{H} = \frac{H}{2L}\left(\sqrt{1+\frac{2GV_0^2L}{BH^3\sigma_d}}-1\right), \tag{23}$$

which takes into account finite displacements.[1] The dynamic flow stress in this equation, σ_d, comes from Eq. (5), whose strain rate is given in Alves and Jones (2002a) as

$$\dot{\varepsilon}_{eq} = \frac{V_0}{L_1}\sqrt{(9/8)\left(1+\xi^2\right)^2h^2+8k^2/3}, \tag{24}$$

which reduces to

$$\dot{\varepsilon}_{eq} = \frac{V_0}{L}\sqrt{9h^2/2+8k^2/3}, \tag{25}$$

when the mass hits the middle ($\xi = 1$) and where $h = H/L$, with $k = 0.26$ being a constant which takes transverse shear into account, assumed here to be the same for both materials.

In order to apply the correction procedure for a given test configuration where the prototype response due to an impact velocity V_{0_p} is desired, it is necessary to calculate β_{V_0}. This should be different from 1 since

[1] The term $2GV_0^2L/BH^3\sigma_d$ can be reduced to GR_n/m_b where $R_n = \rho V_0^2L^2/\sigma_0H^2$ is the Zhao dimensionless number (Zhao, 1998) with m_b being the beam mass.

Table 3
Material properties for the prototype and models

Mild steel prototype	Aluminium models
$E = 200$ GPa	$E = 72$ GPa
$\rho = 7800$ kg/m^3	$\rho = 2800$ kg/m^3
$\sqrt{E/\rho} = 5063$ m/s	$\sqrt{E/\rho} = 5070$ m/s
$\sigma_{s_p} = 235$ MPa	$\sigma_{s_m} = 135$ MPa
$q_p = 5$	$q_m = 4$
$D_p = 40$/s	$D_m = 1{,}288{,}000$/s

there is a distortion in the scaling laws due to the different materials used or to strain rate effects. One now simply uses Eqs. (11) and (20),[2] with the strain rate given by Eq. (25), so the new impact velocity, V_{0_m}, is obtained. This is then used in Eq. (23) to obtain the new corrected scaled displacement.

3.1. Results

Fig. 5(a) shows the dimensionless maximum beam displacement for prototype and models when no correction procedure whatsoever is adopted. The prototype beam is $2L = 100$ mm long, with $B = 7.94$ mm, $H = 8.84$ mm, subjected to an impact velocity of 50 m/s by a mass of 6.5 kg. It is evident that the models, scaled by $\beta = 1/2, 1/4, 1/10, 1/20$, are rather distorted in relation to the prototype in the sense that the higher the impact velocity, V_0, and the smaller the scaling factor β, the larger the difference between the dimensionless mid-displacement of models and prototypes.

On the other hand, Fig. 5(b) shows the same dimensionless mid-span beam displacement for the mild steel prototype and for the aluminium-like models but now subjected to the correction outlined before. It is rather evident and convincing that models and prototypes behave all the same; the error in this case is zero.

4. Clamped beam subject to a uniformly distributed velocity pulse

The problem in this section is of a beam loaded with an initial impact velocity throughout all its span (Fig. 6). Different phases of motion exist for this problem, as detailed by Jones (1989), and of interest here is the final maximum displacement achieved by the prototype and the model.

The final displacement for this class of beams, W_f, reads

$$\frac{W_f}{H} = \frac{1}{2}\left[(1 + 3\lambda/4)^{1/2} - 1\right], \tag{26}$$

where H is the beam depth and

$$\lambda = \frac{4\rho V_0^2 L^2}{\sigma_s H^2} \tag{27}$$

is a dimensionless impact energy which can also be related to the dimensionless number R_n discussed elsewhere (Zhao, 1998; Jacob et al., 2004; Li and Jones, 2000).

[2] The same results can be obtained by using Eq. (22) since D_m is very large.

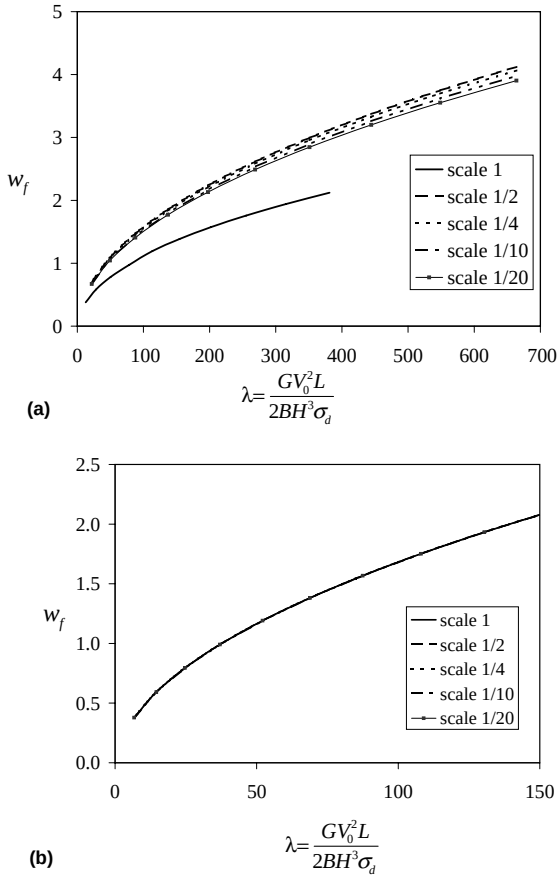

Fig. 5. Dimensionless maximum mid-displacement evolution of a clamped beam hit by a drop mass versus the dimensionless impact energy. The prototype and the model have mechanical strengths typical of mild steel and aluminium, respectively: (a) no correction and (b) corrected solution.

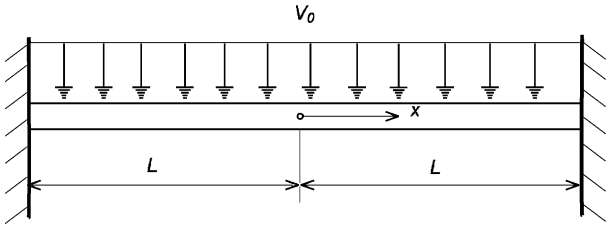

Fig. 6. A clamped beam under a transverse blast load.

It can be shown (Alves and Jones, 2002a) that Eq. (26) becomes

$$\frac{W_f}{H} = \frac{1}{2}\left[\left(1 + \frac{3\rho V_0^2 L^2}{n\sigma_s H^2}\right)^{1/2} - 1\right] \tag{28}$$

when strain rate effects are taken into account with the Cowper–Symmonds equation, where

$$n = \frac{\sigma_d}{\sigma_s} = 1 + \left(\frac{V_0 W_f}{3\sqrt{2}DL^2}\right)^{1/q}, \tag{29}$$

since the strain rate in this beam is

$$\dot{\varepsilon} = \frac{V_0 W_f}{3\sqrt{2}L^2}. \tag{30}$$

Observe that scaled beams would have the same scaled final mid-span displacement according to Eq. (28) if it were not for the strain rate sensitivity factor, n, which, when scaled, gives

$$n = 1 + \left(\frac{V_0 W_f}{3\sqrt{2}D\beta L^2}\right)^{1/q}. \tag{31}$$

It is clear from Eq. (31) that the scale factor, β, cannot be eliminated, which makes Eq. (28) β dependent. Accordingly, the model response will be distorted in relation to the prototype, which prompts one to apply the correction procedure outlined before. By doing so, it is possible to scale the beam response even on the extreme case of models and prototypes being made of different materials.

4.1. Correction procedure and results

The correction procedure is rather simple to be applied and it consists in obtaining the new scaling factor β_{V_0} from Eq. (19)

$$\beta_{V_0} = \sqrt{\frac{f(\beta_{V_0}\dot{\varepsilon}_m^{nc})}{f(\beta\dot{\varepsilon}_m^{nc})}}, \tag{32}$$

where the non-correct strain rate for the model, from Eq. (30), is

$$\dot{\varepsilon}_m^{nc} = \frac{V_0 W_{f_m}^{nc}}{3\sqrt{2}L_m^2}. \tag{33}$$

This yields

$$\beta_{V_0} = \sqrt{\frac{\sigma_{0_m}\left[1 + \left(\frac{\beta_{V_0} V_0 W_{f_m}^{nc}}{3\sqrt{2}DL_m^2}\right)^{1/q}\right]}{\sigma_{0_p}\left[1 + \left(\frac{\beta V_0 W_{f_m}^{nc}}{3\sqrt{2}DL_m^2}\right)^{1/q}\right]}}, \tag{34}$$

which can be solved numerically to give β_{V_0}.

Table 4 lists the various velocity factors used for each model in order to obtain a final dimensionless mid-span beam displacement with errors smaller than 2.7%.

Table 4
Results for the beam under an impulsive load

β	β_{V_0}	W_f/H	Error (%)
1	–	4.3873	–
1/2	0.5491	4.2691	2.7
1/4	0.5533	4.2753	2.6
1/10	0.5600	4.2848	2.3
1/20	0.5661	4.2930	2.2

5. Double plate under axial impact

The last application considers the axial impact of a mass on the double plate structure shown in Fig. 7. This problem was chosen because it is particularly very sensitive to strain rate effects and it was explored at length by Calladine and collaborators (Calladine and English, 1986; Tam and Calladine, 1991) and by Zhang and Yu (1989). It consists of two plates clamped together at the base and at the top. The plates were pre-bent by a small initial rotation and axially impacted by a mass, G, travelling with an initial velocity, V_0.

Suppose the test will be performed in a small scale model made of aluminium and from the model response one intends to obtain the actual response of a mild steel double plate prototype.

The model in Fig. 7 has two phases of motion which were described by Tam and Calladine (1991), Zhang and Yu (1989) and further detailed by Oshiro and Alves, 2004 and Alves and Oshiro (in press) in the scaling context. There is an initial phase of motion where the plates are compressed as described by the shortening s,

$$V_0 - (S\sigma_d/G)t = 2\left(\frac{12\sigma_d S}{ml}\right)^{1/2}\frac{w_0^2}{l}\sinh\left[2\left(\frac{12\sigma_d S}{ml}\right)^{1/2}t\right] + \dot{s}, \tag{35}$$

which ends at $t = \tau_1$ when $\dot{s} = 0$, where S is the cross-section of the bar, $l = 2L$, m is the mass of the bars and w_0 is the horizontal displacement at the center of the bars corresponding to the initial rotation, θ_0. σ_d is the dynamic flow stress obtained using the Cowper–Symmonds equation. The final rotation and angular velocity at this first phase of motion are given by

$$\theta_1 = \frac{2}{l}w_0\cosh\left\{\sqrt{\frac{12S\sigma_d}{ml}}\tau_1\right\} \quad \text{and} \quad \dot{\theta}_1 = \frac{2}{l}w_0\sqrt{\frac{12S\sigma_d}{ml}}\sinh\left\{\sqrt{\frac{12S\sigma_d}{ml}}\tau_1\right\}, \tag{36}$$

which are used as the initial conditions for the second (bending) phase of motion ruled by

$$\ddot{\theta} + \frac{L^2(m+G)\sin\theta\cos\theta\dot{\theta}^2 + M_1 + M_2}{L^2\left[m/3 + (m+G)\sin^2\theta\right]} = 0, \tag{37}$$

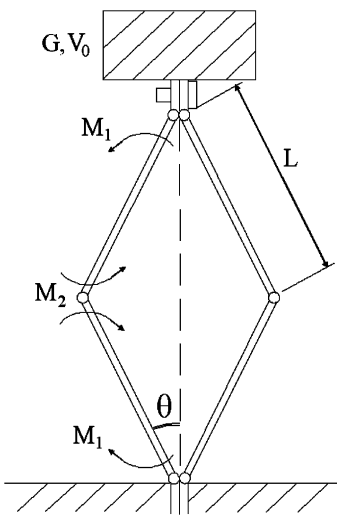

Fig. 7. A two-plate structure under an axial impact.

possible to be solved numerically when adopting

$$M_1 = \left[\left(\frac{\dot{\theta}}{8D}\right)^{1/p}\frac{2p}{2p+1}+1\right]M_s \quad \text{and} \quad M_2 = \left[\left(\frac{\dot{\theta}}{4D}\right)^{1/p}\frac{2p}{2p+1}+1\right]M_s, \tag{38}$$

where $M_s = \sigma_s bh^2/4$, is the bending moment, b and h are the plate width and thickness and a hinge length of $4h$ was adopted (Tam and Calladine, 1991).

If one tries to scale these equations by β, we notice at once that they cannot obey the scaling laws due to the fact that the constants D and q as well as the static flow stress, σ_s, are different in the model and in the prototype.

By numerically solving the governing equation, one can obtain the evolution of the rotation angle, θ, as shown in Fig. 8(a), for different scaling factors, when the model is made of an aluminium material and the prototype made of steel. It is evident and expected that the angular motion for the various scaling factors does not collapse in a single curve, as one would wish in an experimental programme, the reason being, of course, that different materials are used for the model and the prototype.

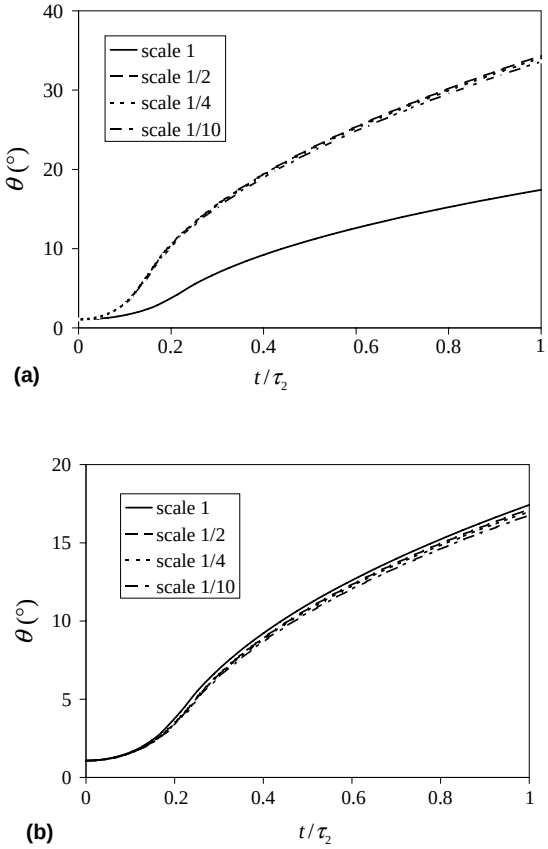

Fig. 8. Lateral plate movement as given by the rotation angle, θ, with dimensionless time for different scaling factors: (a) no correction for distortion has been applied and (b) correction applied. The prototype is made of mild steel and the models of aluminium.

5.1. Correction procedure and results

We now seek a new impact velocity which, when applied to the aluminium models associated with the various scaling factors, will yield the same scaled behaviour as for the mild steel prototype. To this end, the equation of motions (35) and (37) are solved initially with no correction whatsoever, i.e. $\beta_{V_0} = 1$.

$\dot{\theta}^{nc}$ at the end of the motion is then used in Eq. (32), which becomes

$$\beta_{V_0} = \left\{ \frac{\sigma_{0_m}\left[\left(\beta_{V_0}\frac{\dot{\theta}^{nc}}{4D_m}\right)^{1/q_m}\frac{2q_m}{2q_m+1}+1\right]}{\sigma_{0_p}\left[\left(\beta\frac{\dot{\theta}^{nc}}{4D_p}\right)^{1/q_p}\frac{2q_p}{2q_p+1}+1\right]} \right\}^{1/2} \tag{39}$$

for the present case. This allows the calculation of β_{V_0} to be used in all the scaled equations of motion and in the dynamic flow stress

$$\sigma_d = \sigma_s\left(1+\frac{\beta_{V_0}V_0}{D\beta l}\right)^{1/q} \tag{40}$$

presented in the (scaled) initial conditions for the second phase of motion (Eq. (36)) (Oshiro and Alves, 2004).

The evolution of the rotation angle, θ, for double plate prototype and models made from the materials in Table 3 hit by a 6.41 kg mass and with the dimensions $L = 25$ mm, $h = 1.6$ mm, $b = 5.0$mm and $\theta_0 = 1.07°$ are shown in Fig. 8(a) for different scaling factors. It is evident that the angular motion is sensitive to the scaling factor since the model and the prototype are made of different materials.

Table 5
Results at the end of the motion for corrected, c, and non-corrected, nc, models with a strength of an aluminium alloy

Variable	$\beta = 1$	$\beta = 1/2$	$\beta = 1/4$	$\beta = 1/10$
β_{V_0}	1.00	0.5430	0.5428	0.5426
θ^c (°)	17.4	17.1	17.0	16.8
θ^{nc} (°)	17.4	34.3	34.0	33.6
Error^c (%)	0.0	1.6	2.5	3.8
Error^{nc} (%)	0.0	97.0	95.4	92.9
τ_1^c (ms)	0.510	0.599	0.491	0.480
τ_1^{nc} (ms)	0.510	1.76	1.74	1.70
Error^c (%)	0.0	2.3	3.8	6.1
Error^{nc} (%)	0.0	245.2	240.2	232.4
A^c (m/s^2)	12,086	12,372	12,559	12,865
A^{nc} (m/s^2)	12,086	3650	3704	3791
Error^c (%)	0.0	2.4	3.9	6.4
Error^{nc} (%)	0.0	69.8	69.4	68.6
$\dot{\varepsilon}^c$ (1/s)	345	351	353	357
$\dot{\varepsilon}^{nc}$ (1/s)	345	198	199	201
Error^c (%)	0.0	2.4	3.9	6.4
Error^{nc} (%)	0.0	42.7	42.4	41.8
σ^c (MPa)	484	496	503	515
σ^{nc} (MPa)	484	146	148	152
Error^c (%)	0.0	2.4	3.9	6.4
Error^{nc} (%)	0.0	69.8	69.4	68.6

Errors are absolute and relative to the prototype ($\beta = 1$), which is made from a mild steel.

Relative to the mild steel prototype, the observed deviations of the non-corrected aluminium scaled models are listed in Table 5 for various scaling factors and variables of the phenomenon at the end of the motion. The results with the methodology advocated here are also listed in Table 5.

It is evident that the errors in most of the variables were reduced to minimum values and such that the evolution of the plate lateral displacement with time is nearly the same for the various scaling factors used, as indicated in Fig. 8(b). In particular, the maximum error for the rotation angle is 3.8% for the scaling factor $\beta = 1/10$.

6. Discussion

In structural impact, the problem of distortion of the standard scaling laws is a severe limitation for inferring the behaviour of a prototype from the model response. This is mainly due to the material strain rate sensitivity, as clearly indicated in Eq. (7) and Fig. 2. Oshiro and Alves (2004) and Alves and Oshiro (in press) have approached this problem and a methodology which virtually eliminates any distortion of the scaling laws due to material strain rate sensitivity has been suggested and proven to be successful.

In the present article, the alluded methodology was expanded to deal with the case when the model and the prototype are made from different materials. The underlying motivation is that, when working with models which are too small or too large in relation to the prototype, it is rather difficult to ensure that their material properties will be the same, specially the stress–strain curve. Also, small differences in the material behaviour can lead to different structural behaviours, which is critical when dealing with instabilities as in the buckling of shells (Karagiozova and Alves, 2004).

In order to test the methodology developed, three dynamic problems were chosen, i.e. a blast load acting on a beam, the transverse impact of a mass on a beam and the axial impact in a double plate. In all these problems, the prototype behaviour was taken as the reference. Hence, it was our aim to verify whether by knowing the response of the models it would be possible to forecast the prototype response. It is stressed here that two very distinct materials were chosen: for the model, it was aluminium material and for the prototype, it was mild steel.

Accordingly, it has been shown that it is indeed possible to infer the behaviour of a mild steel prototype, even in the extreme case when the models are made of an aluminium alloy. This seems a very important result in the context of the theory of scaling impacted structures. Indeed, it is possible to affirm that the problem of non-scalability of strain rate sensitive structures is now solved, with the additional important advantage that the model and the prototype can be made of different materials.

It is also noticeable from the previous sections that the whole procedure for correction is quite simple in the sense that the corrected loading configuration capable of scaling the structural response can easily be obtained.

It should be indicated that the present methodology has been tested for other cases (Alves and Oshiro, in press; Oshiro and Alves, 2004) and that so far no flaw has been detected. The present methodology has, however, a limitation.

In deriving Eq. (4), it was assumed that the wave speed was the same in the model, c, and in the prototype, C. Otherwise, Eq. (4) would read

$$t = \beta T \frac{C}{c}. \tag{41}$$

So, strictly speaking, Eqs. (4) and (41) lead to different results which, in turn, may affect the model response for cases where elastic effects are important. For the problems analysed here, however, these effects are not taken into account. Also, as indicated in Table 3, $C/c = 0.99$, which ensures the numerical values of Eqs. (4) and (41) to be virtually the same.

In the more general case, an improvement in the present theory is necessary to take this shortcoming into account. This is particularly important in the context of buckling initiation, whose peak load depends on these parameters (Karagiozova et al., 2000).

7. Conclusion

This article shows that it is possible to scale structures subjected to impact loads when their models are made of another material different from the prototype one. For this, a technique based on a new set of dimensionless numbers, coming from a mass, velocity, stress basis rather than the traditional mass, time, length basis, has been used.

It is quite appealing that the models and the prototypes can be constructed from different materials. This substantially facilitates the task of crafting models similar to the prototype.

Hence, it is possible from the present theory to make a plastic model and from its response to infer the behaviour of a metal prototype, at least for the case when elastic effects are secondary. The various benefits one can obtain with the approach discussed here are enormous and even with dissimilar materials the scalability of a structure can be guaranteed within a very small error.

The approach is simple, robust and accurate and such that the problem of non-scalability of dissimilar model and prototype material strengths is no longer an unsolved one.

References

Alves, M., 2000. Material constitutive law for large strains and strain rates. Journal Engineering Mechanics 126 (2), 215–218.

Alves, M., Jones, N., 2002a. Impact failure of beams using damage mechanics: Part I—Analytical model. International Journal of Impact Engineering 27 (8), 837–861.

Alves, M., Jones, N., 2002b. Impact failure of beams using damage mechanics: Part II—Application. International Journal of Impact Engineering 27 (8), 863–890.

Alves, M., Oshiro, R., in press. Scaling the impact of a mass on a structures. International Journal of Impact Engineering.

Baker, W., Westine, P., Dodge, F., 1991. Similarity Methods in Engineering Dynamics. Elsevier.

Booth, E., Collier, D., Miles, J., 1983. Impact scalability of plated steel structures. In: Jones, N., Wierzbicki, T. (Eds.), Structural Crashworthiness. Butterworths, London, pp. 136–174.

Calladine, C., English, R., 1986. Strain rate and inertia effects in the collapse of two types of energy-absorbing structure. International Journal of Mechanical Sciences 26, 689–701.

Duffey, T., Cheresh, M., Sutherland, S., 1984. Experimental verification of scaling laws for punch-impact-loaded structures. International Journal of Impact Engineering 2 (1), 103–117.

Hu, Y., 2000. Application of response number for dynamic plastic response of plates subjected to impulsive loading. International Journal of Pressure Vessels and Piping 77, 711–714.

Jacob, N., Yuen, S., Nurick, G., Bonorchis, D., Desai, S., Tait, D., 2004. Scaling aspects of quadrangular plates subjected to localised blast loads—experiments and predictions. International Journal of Impact Engineering 30 (8–9), 1179–1208.

Johnson, W., 1973. Impact Strength of Materials. Edward Arnold, London.

Jones, N., 1984. Scaling of inelastic structures loaded dynamically. In: Davies, G. (Ed.), Structural Impact and Crashworthiness. Elsevier Applied Science, pp. 45–74.

Jones, N., 1989. Structural Impact. Cambridge University Press, Cambridge.

Jones, N., Jouri, W., Birch, R., 1984. On the scaling of ship collision damage. In: Third International Congress on Marine Technology, Athens, pp. 287–294.

Karagiozova, D., Alves, M., 2004. Transition from progressive buckling to global bending of circular shells under axial impact—Part I: Experimental and numerical observations. International Journal of Solids and Structures 41 (5–6), 1565–1580.

Karagiozova, D., Alves, M., Jones, N., 2000. Inertia effects in axisymmetrically deformed cylindrical shells under axial impact. International Journal of Impact Engineering 24 (10), 1083–1115.

Li, Q., Jones, N., 2000. On dimensionless number for dynamic plastic response of structural members. Archive of Applied Mechanics 70, 245–254.

Liu, J., Jones, N., 1988. Dynamic response of a rigid plastic clamped beam struck by a mass at any point on the span. International Journal of Solids and Structures 24 (3), 251–270.

Nurick, G., Martin, J., 1989. Deformation of thin plates subjected to impulsive loading—a review, Part II: Experimental studies. International Journal of Impact Engineering 8, 171–186.

Oshiro, R., Alves, M., 2004. Scaling impact structures. Archive of Applied Mechanics 74, 130–145.

Shi, X., Gao, Y., 2001. Generalization of response number for dynamic plastic response of shells subjected to impulsive loading. International Journal of Pressure Vessels and Piping 78, 453–459.

Tam, L., Calladine, C., 1991. Inertia and strain-rate effects in a simple plate structure under impact loading. International Journal of Impact Engineering 11, 349–377.

Wen, H., Jones, N., 1993. Experimental investigation of the scaling laws for metal plates struck by large masses. International Journal of Impact Engineering 13 (3), 485–505.

Zhang, T., Yu, T., 1989. A note on a velocity sensitive energy-absorbing structure. International Journal of Impact Engineering 8, 43–51.

Zhao, Y., 1998. Suggestion of a new dimensionless number for dynamic plastic response of beams and plates. Archive of Applied Mechanics 68, 524–538.